JOURNAL OF MATERIALS SCIENCE 31 (1996) 4039–4046

Structural evolution of matrix phase for liquid phase sintered 93W–4.9Ni–2.1Fe

Y. H. CHIOU, Y. S. ZU, S. T. LIN
Mechanical Engineering Department, National Taiwan Institute of Technology, Taipei, Taiwan

The structure of the matrix of a two phase heavy alloy, 93W–4.9Ni–2.1Fe (wt %), was characterized. The matrix phase was not the expected face centred cubic Ni–Fe–W solid solution with a large grain size reported in the literature. Instead, an amorphous phase containing fine grained crystals as well as intermetallic compounds having different compositions were found. The partition of tungsten from the matrix toward the tungsten phase resulted in formation of different phases in the matrix. Under furnace cooling, the matrix phase was composed of an amorphous phase for the matrix phase remote from the tungsten grain–matrix interfaces, and a strained FeNi intermetallic phase near the interfaces. For specimens solution treated at temperatures between 1000–1400 °C followed by water quenching, an intermetallic phase rich in tungsten, (Ni, Fe) W, evolved and surrounded the tungsten grains in clusters. The relative abundance of this intermetallic phase was highest for a solution treatment temperature of 1400 °C, indicating that the formation of this phase was a result of supersaturation of tungsten in the matrix phase and retarded partition of tungsten from the matrix phase to tungsten grains under a rapid cooling condition.

1. Introduction

Tungsten heavy alloys are a class of composites whose microstructures consist of approximately spheroidal tungsten grains imbedded in a ductile nickel based matrix phase. The compositions of the tungsten heavy alloys are either W–Ni–Fe or W–Ni–Cu, with W–Ni–Fe being found to have the better mechanical properties [1–3]. The W–Ni–Fe alloys usually contain 80 to 98 wt% of tungsten, and an optimal nickel to iron ratio of 7:3 as the rest [1, 4]. Typical applications of this class of alloys include kinetic energy penetrator, shaped charge liner, inertial counter weight balance, and radiation shield [5].

The complexity of the factors influencing the toughness of liquid phase sintered tungsten heavy alloys had been summarized elsewhere [2, 3, 6]. Considerable effort has been made to improve the mechanical properties such as ductility and toughness by various heat treatment approaches. However uncertainties regarding the heat treatment effect on the mechanical properties of the tungsten heavy alloys still remain. For example, both rapid cooling by water quenching following solution treatment [1, 4, 6, 7] and slow furnace cooling [1, 8–10] after sintering were reported to improve the ductility and toughness. Though a rapid cooling heat treatment was generally believed to improve the mechanical properties of heavy alloys, different explanations regarding its effect have been proposed. German *et al.* [6] had compiled a list of publications that have proposed explanations for the cooling rate effect on the ductility or toughness of tungsten heavy alloys. These proposed explanations included impurity segregation to interfaces, compositional and heat treatment effects on the matrix phase and tungsten grain chemistry, hydrogen embrittlement of the matrix phase, formation of intermetallic compounds, changes in pore structure, and a ductile to brittle transition close to room temperature. The underpinning approach for most of these reports was that attention was focused on the tungsten grain–matrix phase interfaces. Hydrogen, impurity, and precipitated intermetallic phases were generally believed to embrittle the alloys by providing a low energy fracture path along the interphase boundaries.

With respect to the structure and composition of the matrix phase, uncertainties remained. It was commonly encountered that only the interfaces between tungsten grains and the matrix phase could be observed in the microstructure while no grain boundary within the matrix could be revealed, a result ascribed to the lack of a reagent for the simultaneous etching of the two phase alloys [9]. Though the microstructural details of the matrix phase were difficult of disclose metallographically, it was popularly believed that the matrix phase was a face-centred cubic (fcc) Ni–Fe–W solid solution [6, 8], having an average grain size of more than 100 μm [11], or 40–100 μm for slow cooling ($< 5\,^{\circ}C\,min^{-1}$) and 3–8 mm for fast cooling ($> 600\,^{\circ}C\,min^{-1}$) [12].

The present research was undertaken to investigate the microstructural details of the matrix phase for furnace cooled and water quenched tungsten heavy alloys. The evolution of the matrix phase associated with the partition of tungsten is demonstrated and

0022–2461

TABLE I. Some characteristics of the starting powders

	Tungsten	Nickel	Iron
Vendor	Korea Tungsten	Novamet	BASF
Grade	KM–8	Inco 4SP	OM
Average Particle Size (μm)	6	11	4
Tap Density ($g\,cm^{-3}$)	2.8	4.7	4.3
Purity (wt %.)	99.95	99.8	97.8
Major Impurities (wt %)	O 0.08	O 0.02 C 0.05 Fe0.01 S 0.001	O 0.30 C 0.89 N 0.90

controlling the mechanical properties by modifying the chemistry and structure of the matrix phase is suggested.

2. Experimental procedure

The heavy alloy used in this study was 93W–4.9Ni–2.1Fe by weight. Some characteristics and micrographs of the powders are shown in Table I, and Fig. 1, respectively. The powders were blended and milled in a plastic jar for 24 h, using 304 stainless steel balls (diameter = 3 mm). The specimens were prepared by injection moulding. The binder was composed of polypropylene (20 wt %), ethylene vinyl acetate (25 wt %), paraffin wax (50 wt %), and stearic acid (5 wt %). The powder-binder blend, which had a powder volume fraction of 0.5, was prepared with a Z-blade mixer at 180 °C for about 80 min. Rectangular test specimens having the dimensions of $70 \times 12 \times 4$ mm were moulded using a reciprocating screw injection moulding machine. The moulded specimens were immersed in heptane to partially remove the paraffin wax and stearic acid [13], which reduced the possibility of forming defects in the following thermal treatment.

A sintering schedule combined with thermal debinding was conducted in a horizontal tube furnace. Post sintering heat treatments of the sintered specimens was carried out for some specimens by solution treating the sintered specimens at temperatures of 1000, 1200, and 1400 °C for 1 h, followed by water quenching. The sintering and heat treatment schedules, as well as the atmosphere, are shown in Fig. 2. A sintering temperature ranging from 1480–1520 °C and a sintering period from 20–60 min were employed for the sintering study. The specimens were furnace cooled. It took approximately 6 h for the specimens to reach temperatures lower than 100 °C. A dry hydrogen atmosphere was used during debinding and sintering until the last 10 min of the isothermal hold when the atmosphere was changed to dry argon [14]. A subsequent heat treatment for some of the specimens was also carried out in argon. The time spent in introducing the heated specimens into the cold water was less than 10 s.

No significant carbon was introduced by the use of carbonyl nickel and iron powders, and the existence of

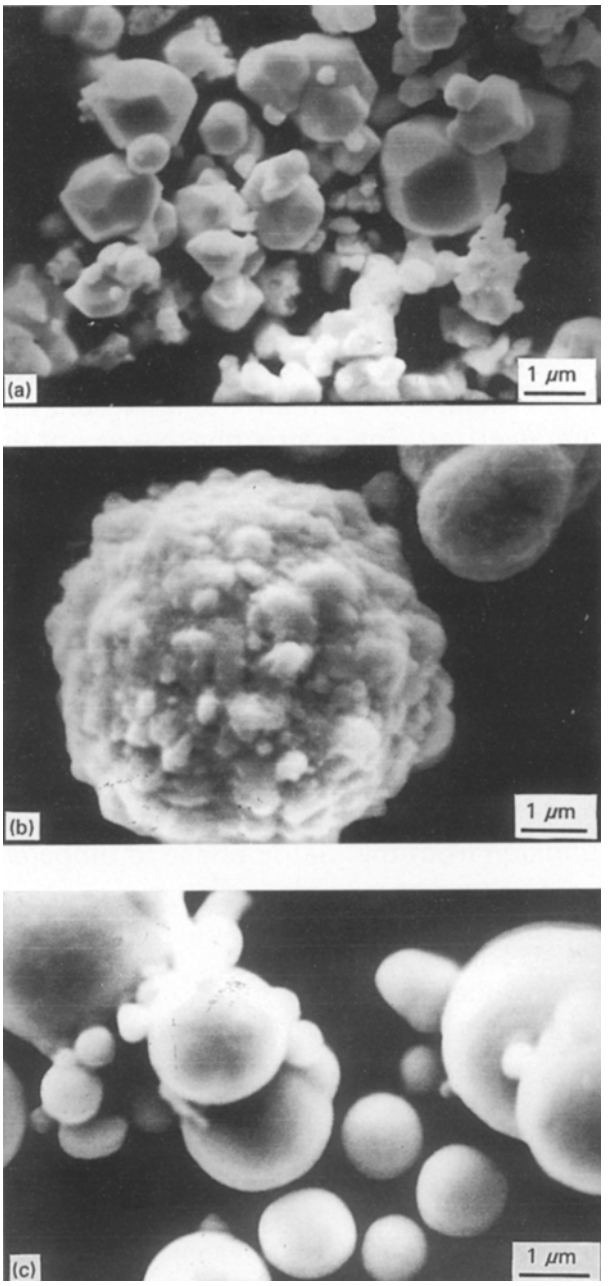

Figure 1 Morphologies of the starting powders, (a) tungsten, (b) carbonyl nickel, and (c) carbonyl iron.

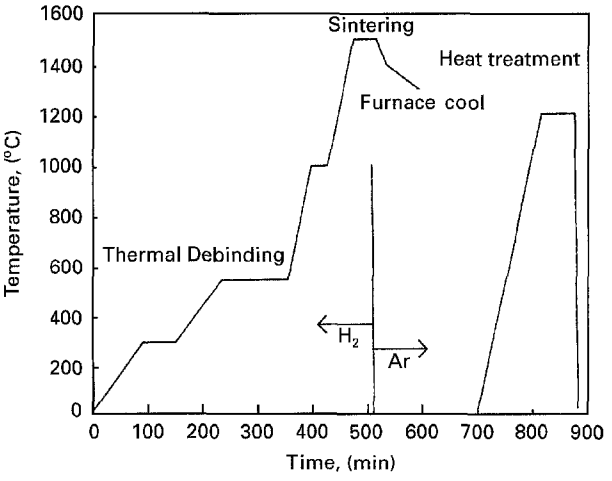

Figure 2 Processing cycles and atmospheres for debinding, sintering and heat treatment.

a large quantity of the organic binder in the green state. The average carbon content of the sintered specimens was 56 ppm, based on nine specimens tested by the combustion method. This average value was lower than the minimum required for forming η carbide precipitate (> 100 ppm) [11].

Both an optical microscope and a scanning electron microscope (SEM, Cambridge S360) were used for morphology analysis. Quantitative analysis of the elements in the matrix phase was carried out using electron probe microanalysis (EPMA), using a Jeol, JAX 8800M attachment under an accelerating voltage of 20 keV. Recorded intensities of Ni K_α, Fe K_α, and W L_α radiations were employed for calculating Ni, Fe, and W concentrations in the phase components. Phase analysis of the bulk sintered specimens was carried out using X-ray diffraction (XRD) using a Rigaku D MAX B diffractometer with Cu K_α radiation at an accelerating voltage of 40 keV. The heat treated specimens were ground to near the centre of the specimens prior to the XRD testing. Microanalysis of the morphology, composition, and structure of the matrix phase was conducted using a scanning transmission electron microscope (STEM), with a Jeol 2000 FX microscope at an accelerating voltage of 200 keV. Energy dispersive X-ray (EDX) analysis spectra and selective area electron diffraction patterns were recorded from the intergranular matrix phase using the conventional transmission mode of operation. Specimens for STEM were prepared by mechanically grinding to a thickness of about 0.5 mm, dimple grinding to a thickness of about 20 μm, and then ion beam thinning until perforation.

3. Results and discussion

3.1. Furnace cool

Fig. 3 shows the XRD patterns of furnace cooled tungsten heavy alloys after sintering at different temperatures (1480–1520 °C) for different sintering times (20–60 min). In addition to the diffraction peaks of the tungsten phase, some peaks having low intensities were also recorded in these patterns, particularly for specimens subjected to an extended sintering time or an elevated sintering temperature. The phase responsible for these low intensity peaks was identified as an FeNi intermetallic phase (fcc, $a = 0.36032$ nm) [15]. In comparison, a crystalline phase having an fcc structure and a lattice parameter in the neighbourhood of 0.360 nm was usually assigned as a Ni–Fe–W solid solution [3, 6, 11, 12, 16].

The lack of diffraction peaks of the fcc Ni–Fe–W solid solution and the varying intensities of the FeNi phase in the XRD patterns shown in Fig. 3 implied the possible existence of an amorphous instead of crystalline Ni–Fe–W phase in the matrix, in addition to the FeNi intermetallic phase identified. Fig. 4 shows STEM micrographs from different locations in the matrix phase for a specimen sintered at 1520 °C for 40 min. Distinct morphological variations in the matrix can be clearly observed in these micrographs. Extensive precipitation occurred near the tungsten grain–matrix interfaces Figs 5 and 6 show the selected area electron diffraction patterns of locations having different morphologies in the matrix phase. These patterns represented an amorphous phase, fine grain crystals crystallizing from an amorphous phase, and

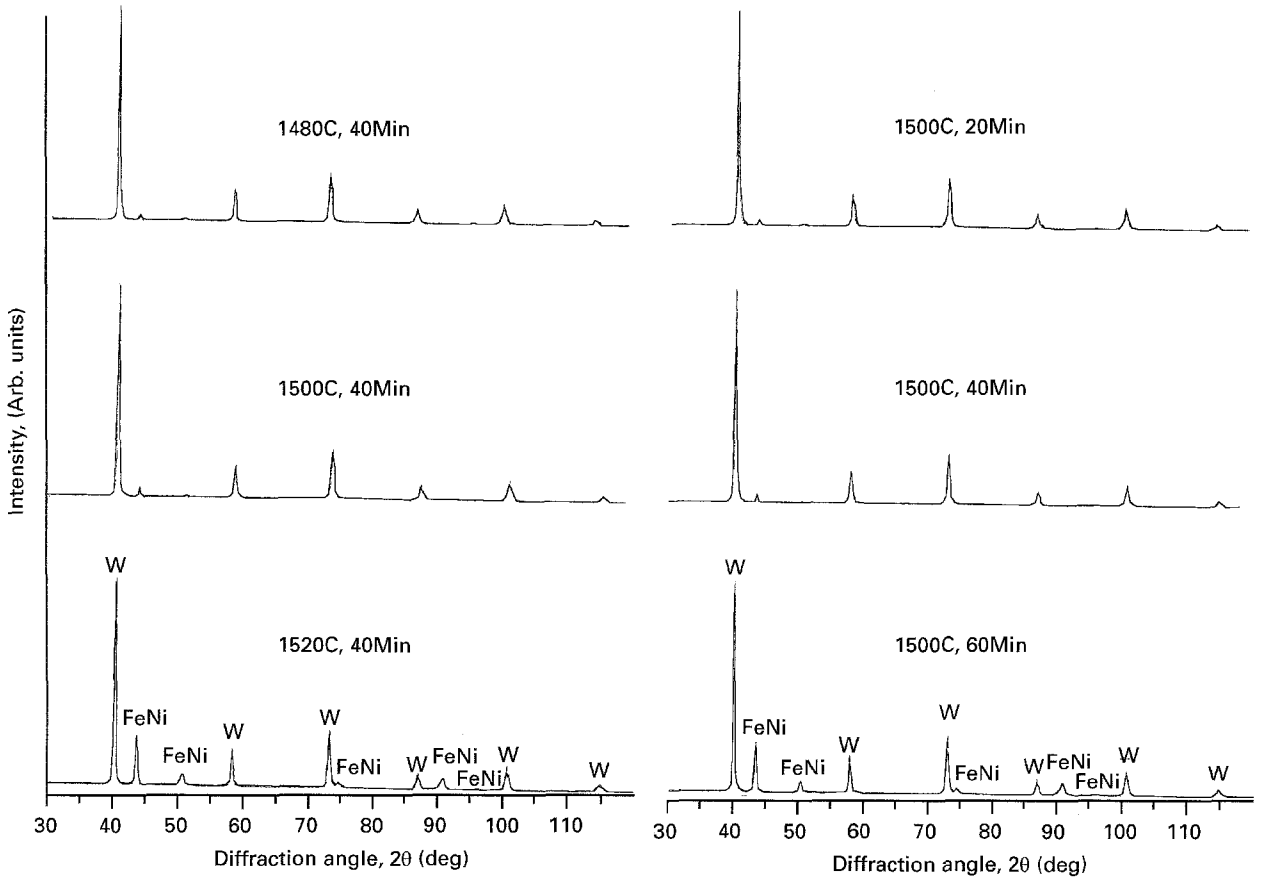

Figure 3 X-ray diffraction patterns for specimens sintered at different temperatures (1480–1520 °C) and for different isothermal holding times (20–60 min).

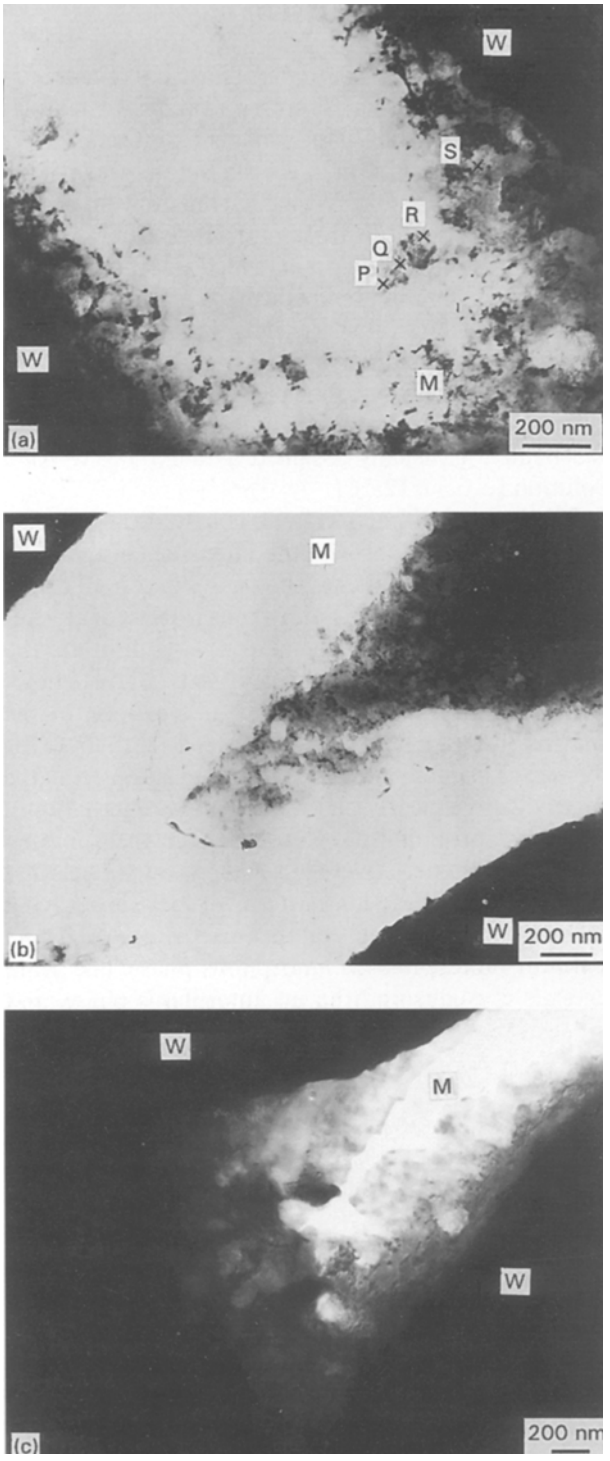

Figure 4 Scanning transmission electron micrographs of the matrix phase located among tungsten grains. The matrix phase is indicated by M and the tungsten phase by W. Microanalyses of structure and composition were carried out near the positions indicated by P, Q, R and S. The sample was sintered at 1520 °C for 40 min.

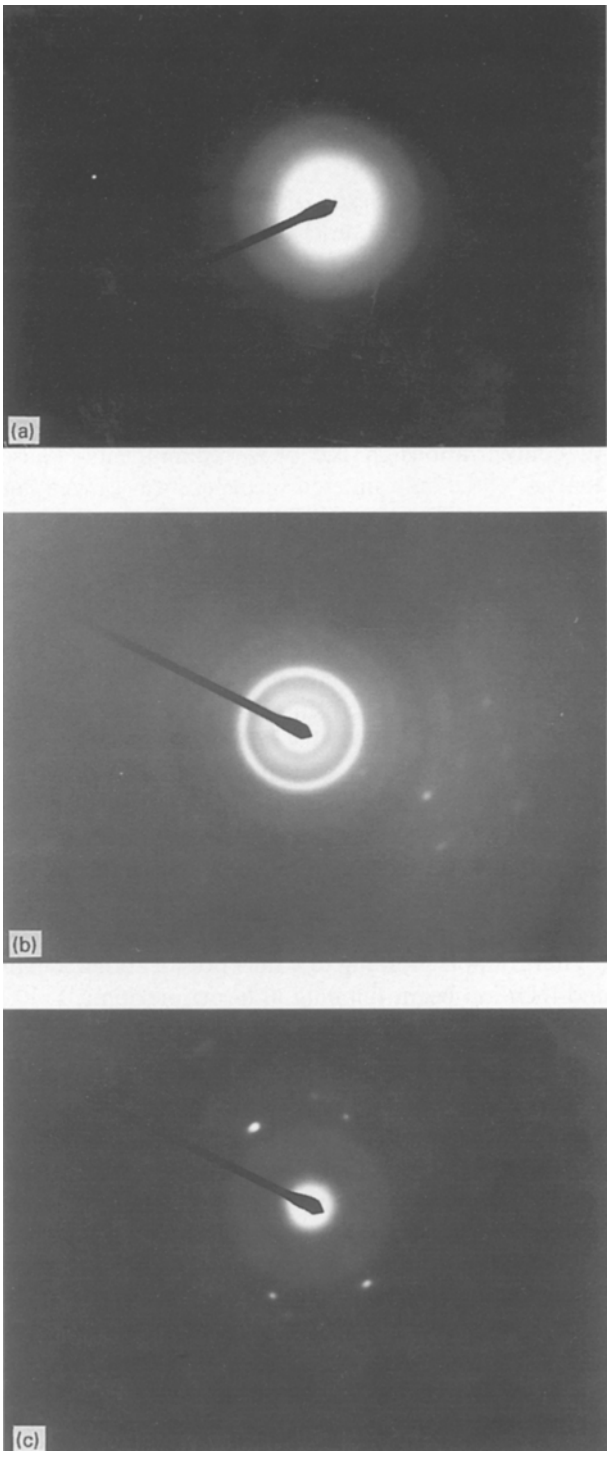

Figure 5 Selected area electron diffraction pattern near the positions P, Q, and R indicated in Fig. 4, representing an amorphous phase (P), fine grain crystals crystallizing from an amorphous phase without preferred grain orientation (Q), and fine grain crystals crystallizing from an amorphous phase with preferred grain orientation (R). (Accelerating voltage = 160 keV, camera length = 60 cm for P and Q, = 100 cm for R).

a crystalline phase, respectively. The crystalline phase located near the tungsten–matrix interfaces was identified as an fcc crystal having a lattice constant of 0.360 $\pm$ 0.001 nm, very close to that ($a = 0.3603$ nm) of FeNi. However, the diffraction patterns of this crystal phase were composed of short arcs rather than sharp spots. This phenomenon indicated the possible existence of strain in the FeNi lattice caused by the dissolved tungsten.

Fig. 7 shows the concentration profile of tungsten in the matrix phase with respect to the distance from the tungsten grain surface. The concentration of tungsten in the matrix phase was position dependent. The amorphous phase was rich in tungsten while the FeNi phase was deficient in tungsten. Indirect observations regarding the formation of FeNi intermetallic phases reported in the past agree with the above observation.

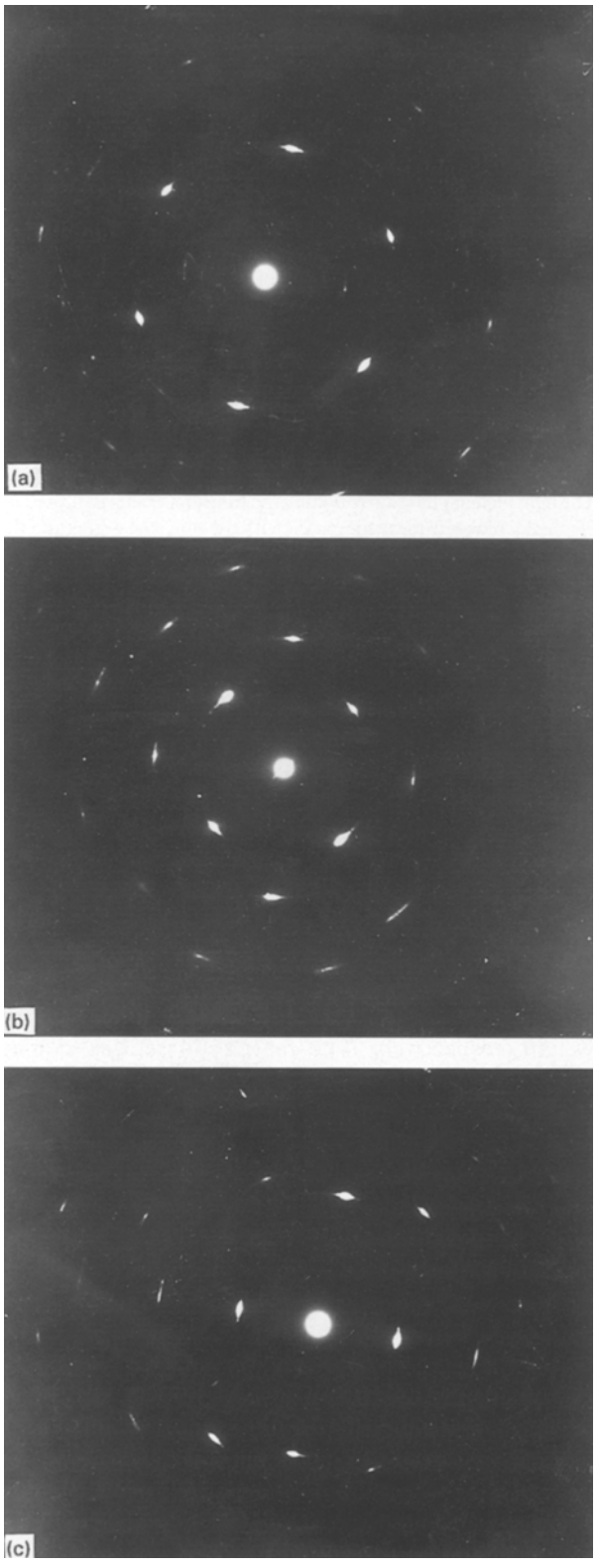

Figure 6 Selected area electron diffraction patterns near the position S indicated in Figure 4, representing (A) (1 1 1) plane, (B) (2 0 0) plane, and (C) (4 2 2) plane of an fcc crystal having a lattice parameter of 0.360 nm. (Accelerating voltage = 200 keV, camera length = 100 cm).

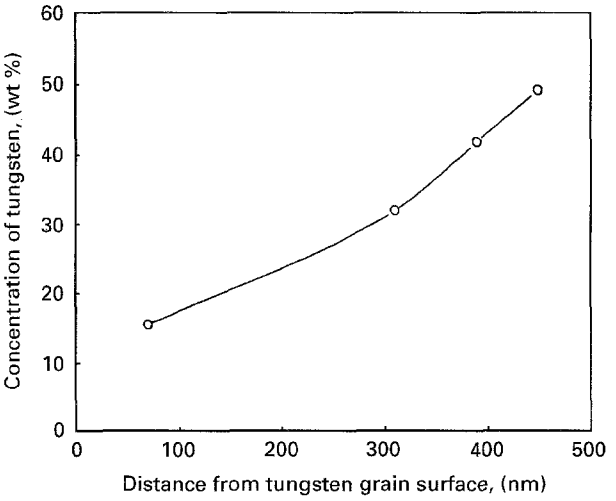

Figure 7 Tungsten concentration profiles in the matrix phase with respect to the distance from the tungsten grain surface, analysed by energy dispersive X-ray analysis.

For example, it was proposed that the formation of intermetallic compounds based on Ni and Fe was favoured by a large binder content or a low tungsten concentration in the matrix phase [17]. Decreasing the cooling rate led to the decomposition of the matrix phase into precipitates near the tungsten grain–matrix interfaces [8], while a precipitate-like phase composed of nickel, iron and possibly tungsten existed in the boundaries between two tungsten grains for furnace cooled heavy alloys [17]. The concentration gradient of tungsten in the matrix phase, shown in Fig. 7, indicated a diffusion event that resulted in the partition of tungsten atoms occurring from the matrix phase toward the tungsten grains. The formation of an FeNi intermetallic phase was thus a result of recovery and recrystallization of the amorphous Ni–Fe–W phase through the repartitioning of tungsten in the matrix [12]. The phase diagram of Fe–Ni indicates the formation of intermetallic phases having different molar ratios of Fe and Ni at temperatures lower than approximately 500 °C [18]. Therefore, a slow furnace cool or a long thermal anneal below this temperature limit could have encouraged the formation of intermetallic phases of Fe–Ni. These phases were located near the tungsten grain–matrix interfaces where depletion of tungsten by precipitating into the tungsten grains was severe. This could have partially contributed to the low impact energy observed for most furnace cooled heavy alloys [1, 4, 6, 7].

The microstructures of tungsten heavy alloys evolved from a mixture of matrix phase and continuous tungsten skeleton at low sintering temperatures to spheroidal tungsten single crystals bounded by an intergranular continuous matrix phase at higher sintering temperatures [2]. During such an evolution event, the morphology of the tungsten phase changed constantly both in grain shape and grain size. Therefore, an intensive dissolution–precipitation event took place in the matrix phase and tungsten concentration gradients existed in the matrix phase. The existence of tungsten concentration gradients in the matrix phase was hardly mentioned in past reports, even though the existence of a tungsten concentration gradient in the matrix phase is fundamental for densification and grain growth of tungsten. Most past reports indicated that the composition of the matrix phase was very consistent irrespective of the sintering parameters or heat treatment history. For example, the matrix phase

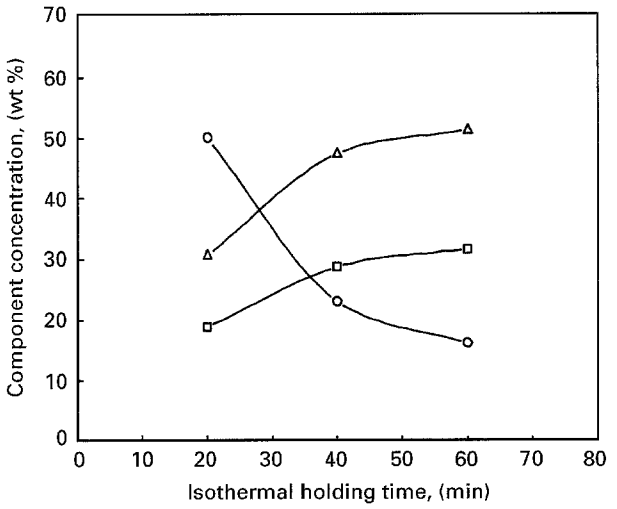

Figure 8 Variation of the matrix phase composition with isothermal holding time at 1500 °C. The compositional analysis was based on electron probe microanalysis and is an average value for the matrix phase. The symbols represent; (○) Tungsten, (Δ) Nickel and (□) Iron.

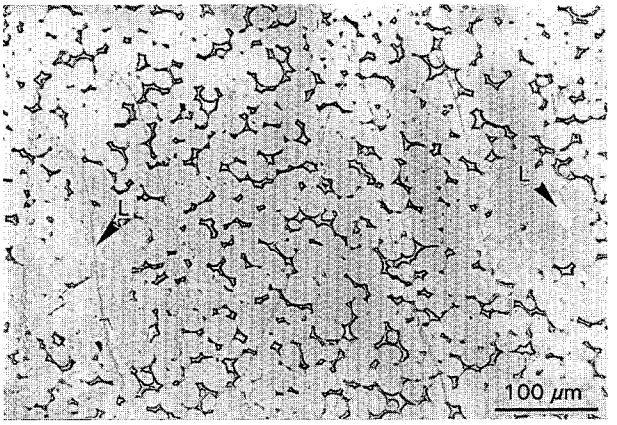

Figure 9 Micrograph for a specimen sintered at 1500 °C for 40 min, followed by solution treatment at 1000 °C and water quenching. The light etched phase surrounding the tungsten grains indicated by "L" had a high hardness compared with the tungsten grains and the matrix phase.

was believed to have a composition in the range of 59Ni–22Fe–19W [6] to 59Ni–26Fe–15W [19], and the maximum solubility of tungsten in nickel and in nickel containing 30 wt% iron were 40 wt% [19] and 30 wt% [2], respectively. However, variation of the composition of the matrix with sintering variables was expected as partition of tungsten occurred constantly. Fig. 8 shows the bulk component concentrations for the matrix phase as a function of isothermal holding time at a sintering temperature of 1500 °C. Therefore, sintering variables substantially affect the structure of the matrix phase through influencing the phase composition. This phenomenon is exemplified by the varying concentrations of the FeNi intermetallic phase shown in Fig. 3.

3.2. Heat treatment

For the specimens water quenched from the solution treatment temperatures of 1000, 1200 and 1400 °C, some bright regions surrounding tungsten grains that were different from the continuous matrix phase were observed. One such observation is shown in Fig. 9 for a specimen sintered at 1500 °C for 40 min followed by solution treatment at 1000 °C for 1 h prior to water quenching. Unlike the other tungsten grains or matrix phase, these regions were difficult to polish and etch. Similar light etched precipitates have been observed elsewhere, but their sizes were much smaller [3, 4]. Nevertheless, it was generally concluded that the microstructures of heavy alloys did not change substantially with heat treatment. Only slight increases in the tungsten concentration in the matrix phase [12, 20], in the matrix phase hardness [6], and in the lattice constant of the matrix phase [12] were observed.

The bright phase was much harder than the tungsten phase or matrix phase. The microhardnesses of the bright phase, tungsten grain, and matrix phase were H_v 1150, H_v 450, and H_v 330 $kg\,mm^{-2}$ respectively. The hardness of this bright phase was much higher than that of Ni–Fe–W phase (H_v 215–254 $kg\,mm^{-2}$) [6], comparable in scale to that of NiW intermetallic phase (H_v 1325 $kg\,mm^{-2}$) [19], but much lower than those of most carbides ($> H_v$ 1600 $kg\,mm^{-2}$) [21]. Additionally, the carbon content of this alloy (< 60 ppm) was lower than the criterion for forming carbides [11]. Therefore, it could not be a solution or carbide of Ni–Fe–W. Quantitative compositional analysis based on EDX indicated that the matrix phase and the bright phase were composed of 51.6Ni–32Fe–16.4W and 14.2Ni–8.8Fe–77 W by weight, respectively. The matrix phase was rich in nickel and iron while the bright phase was rich in tungsten. Since the atomic fraction of tungsten in the bright phase was 0.51, it was plausible that this phase was a (Ni, Fe) W intermetallic phase that had the same crystal structure as NiW [4]. However, a (Ni, Fe) WC carbide phase was proposed for a similar thin bright region located near the tungsten–matrix interfaces [3].

Fig. 10 shows the effect of the solution treatment temperature prior to water quenching on the phase evolution of tungsten heavy alloys sintered at 1500 °C for 40 min, examined using XRD. The development of new phases was evident for specimens subjected to a solution treatment temperature of 1400 °C prior to the water quenching. Attempts to index these low intensity peaks with known compounds in the powder diffraction file [15] failed to identify a single phase. However there was no diffraction pattern for NiW in the file. It should be noted that these peaks had a close match (by a difference of less than 1 °) with those of orthorhombic NiW [19].

Based on the above observations and analyses, the NiW intermetallic phase could have formed when saturation of tungsten in the solid solution occurred. It also might have formed when partition of the tungsten atoms in the matrix phase by precipitating into the tungsten grains was inhibited by a long diffusion distance or a fast cooling rate. Therefore, maintaining the tungsten concentration in the matrix phase to a proper ratio and controlling the partition behaviour

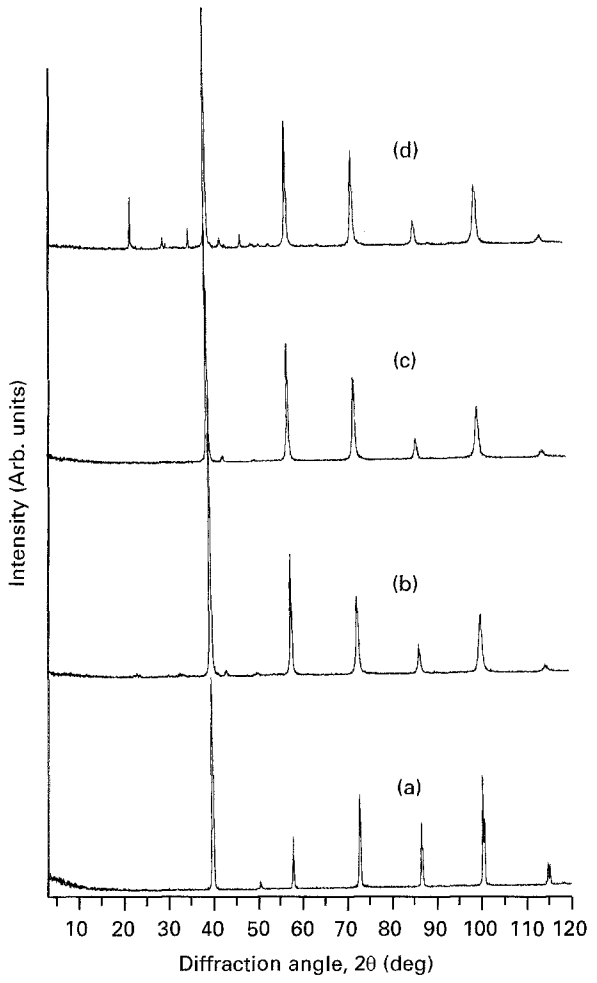

Figure 10 X-ray diffraction patterns for specimens sintered at 1500 °C for 40 min followed by solution treatment at different temperatures and water quenching. The conditions used were (a) 1500 °C, 40 min (b) 1500 °C, 40 min + 1000 °C, WQ (c) 1500 °C, 40 min + 1200 °C, WQ and (d) 1500 °C, 40 min + 1400 °C, WQ.

of tungsten in the matrix during heat treatment are the keys to controlling the structural evolution of the matrix phase.

Maintaining the tungsten concentration in the matrix phase to a proper ratio can be achieved by controlling the sintering profile, as is observed from the variation of matrix phase composition with isothermal holding time shown in Fig. 8. It can also be achieved by adjusting the chemistry of the powder system. For example, the addition of copper to the W–Ni system reduces the solubility of tungsten in the matrix phase to less than 30 wt %, which in turn prevents the formation of the Ni_4W intermetallic phase [1]. A high concentration of carbon in W–C–Ni reduces the concentration of tungsten dissolved into the matrix phase and prevents the formation of the NiW intermetallic phase [22, 23].

The controversial conclusions regarding the effect of cooling rate on the mechanical properties of heavy alloys could have been caused by the different concentrations of tungsten in the matrix phase prior to heat treatment. A variation of the component concentrations as a result of different sintering schedules is shown in Fig. 8. Furthermore, there possibly exists an optimum intermediate cooling rate to avoid the formation of either FeNi or (Ni, Fe) W. The rapid or slow cooling rates defined in past reports that contributed to better mechanical properties could have lain in this optimum range. Based on this argument, a slight difference in the cooling rate can contribute to a significant difference in the toughness of heavy alloys. For example, two batches of rapid water quenched 95W–3.5Ni–1.5Fe, under the assumption of an identical cooling rate, had a significant difference in impact energy, i.e., 81 J versus 18 J [6]. The baseline impact energy was 7 J for the specimens without heat treatment.

4. Conclusions

The structural evolution of the matrix phase in tungsten heavy alloys depended on the sintering and subsequent heat treatment history. An extensive sintering event as a result of an elevated sintering temperature or an extended sintering time followed by furnace cooling promoted the partition of tungsten atoms from the matrix phase toward tungsten grains. Such a behaviour encouraged the crystallization of an FeNi intermetallic phase near the tungsten grain–matrix interfaces at the expense of an amorphous Ni–Fe–W phase. On the other hand, a rapid water quenching subsequent to solution treatment at temperatures between 1000–1400 °C caused crystallization of an (Ni, Fe) W intermetallic phase that has the same lattice structure as NiW. The depletion of tungsten in the matrix phase was responsible for the crystallization of an FeNi intermetallic phase, while supersaturation of tungsten in the matrix phase was a primary cause for the crystallization of the (Ni, Fe) W intermetallic phase.

Acknowledgement

This research was financially supported by the National Science Council, Taiwan, (NSC 82-0405-E011-175), and 204 Arsenal, Ordnance Production Service and Combined Service Force (204-83-98).

References

1. D. J. JONES and P. MUNNERY, *Powder Met.* **10** (1967) 156.
2. W. E. GURWELL, in "Progress in Powder Metallurgy, Vol. 42", edited by E. A. Carlson and G. Gaines (Metal Powder Industries Federation, Princeton, N.J., 1986) p. 569.
3. B. C. MUDDLE, *Metall. Trans. A* **15A** (1984) 1089.
4. D. V. EDMONDS and P. N. JONES, *ibid.* **10A** (1979) 289.
5. W. D. SCHUBERT, *Ref. Metals Hard Mater.* **11** (1992) 151.
6. R. M. GERMAN, J. E. HANAFEE and S. L. DIGIALLONARDO, *Metall. Trans. A* **15A** (1984) 121.
7. B. C. MUDDLE and D. V. EDMONDS, *Metal Sci.* **17** (1983) 209.
8. L. G. BAZHENOVA, A. D. VASIL'EN, R. V. MINAKOVA and V. I. TREFILOV, *Soviet Powder Met. Metal Ceram.* **19** (1980) 34.
9. R. V. MINAKOVA, A. N. PILYANKEVICH, O. K. TEODOROVICH, and I. N. FRANTSEVICH, *ibid.* **7** (1968) 396.
10. *idem. ibid.* **7** (1968) 483.
11. J. B. POSTHILL, M. C. HOGWOOD and D. V. EDMONDS, *Powder Met.* **29** (1986) 45.

12. R. V. MINAKOVA, N. A. STROCHAK, P. A. VERKHOVODOV, L. G. BAZHENOVA and V. L. POLTORATSKAYA, *Soviet Powder Met. Metal Ceram.* **19** (1980) 842.
13. S. T. LIN and R. M. GERMAN, *Powder Met. Int.* **21** (1989) 19.
14. A. BOSE and R. M. GERMAN, *Metall. Trans. A* **19A** (1988) 2467.
15. JCPDS, "Powder Diffraction File Search Manual, Hanawalt Method, Inorganic" (International Center for Diffraction Data, Swarthmore, PA, 1990).
16. A. F. GUILLERMET and L. OSTLUND, *Metall. Trans. A* **17A** (1986) 1809.
17. N. UELNISHI and Y. TAKEDA, in "Tungsten and Tungsten Alloys, Recent Advances", edited by A. Growson and E. S. Chen (The Minerals, Metals and Materials Society, PA, 1991) p. 129.
18. G. V. RAYNOR and V. G. RIVLIN, "Phase Equilibria in Iron Ternary Alloys" (The Institute of Metals, London, 1988), p. 46.
19. J. M. WALSH and M. J. DONACHIE Jr., *Metall. Trans. A* **4** (1973) 2854.
20. C. LEA, B. C. MUDDLE and D. V. EDMONDS, *ibid.* **14A** (1983) 667.
21. H. KNOCH, in "European Symposium on Engineering Ceramics", edited by F. L. Riley (Elsevier Science Publishing Co, New York 1989) p. 151.
22. E. F. DRAKE and A. D. KRAWITZ, *Metall. Trans. A* **12A** (1981) 505.
23. V. A. TRACEY, *Ref. Metals Hard Mater.* **11** (1992) 137.

Received 28 June
and accepted 21 December 1995